*29th EPS Conference on Plasma Phys. and Contr. Fusion Montreux, 17-21 June 2002 ECA Vol. **26B**, O-3.23 (2002)*

Convective Blob Transport and the Density Limit

J. R. Myra, D. A. D'Ippolito

Lodestar Research Corp., 2400 Central Avenue, Boulder, Colorado 80301

S. I. Krasheninnikov, S. A. Galkin

University of California, San Diego, California

A reduced electromagnetic (EM) model for convective blob transport in the scrape-off-layer (SOL) is developed in which the density is naturally normalized to a parameter which has the same B/qR dependence as the Greenwald-Hugill density limit. The model produces qualitative effects which are reminiscent of observed phenomena, but at densities which are well above the experimental density limit

Recent advances in the experimental diagnosis and first principles simulation of edge and SOL plasma in tokamaks and other toroidal devices suggest the importance and possible relationship of convective transport, strong nonlinearities giving rise to intermittency, and the emergence of coherent turbulent structures. Here, we build on Refs. 1 and 2 by generalizing the convective blob transport model to include electromagnetic (EM) effects and investigate how they are related to experimentally observed changes in the SOL near the density limit.[3,4]

In the SOL we estimate the sheath current[5] as $J_\parallel \sim ne^2c_s\phi/T$ and employ it in Ampere's law $A_\parallel \sim 4\pi J_\parallel/ck_\perp^2$ to obtain $A_\parallel \sim \omega_{pi}^2\phi/(cc_sk_\perp^2)$. Further employing $k_\perp\rho_s \sim \varepsilon$ and $\omega/\Omega_i \sim \varepsilon^2$ where ε is an ordering parameter, EM effects will be significant when $A_\parallel \sim (k_\parallel c/\omega)\phi$ which implies

$$L_\parallel \rho_s = \delta_i^2 \tag{1}$$

where $L_\parallel$ is the field line length between the plates in the SOL and $\delta_i = c/\omega_{pi}$ is the ion skin depth. Here $k_\perp$ and ω are a typical wavenumber and frequency, $k_\parallel \sim 1/L_\parallel$, ρ_s is the ion Larmor radius based on the sound speed c_s, and Ω_i is the ion cyclotron frequency.

Equation (1) gives the characteristic density at which EM effects enter as $n_e = 5.06 \times 10^{20}\, \mu^{1/2}B/(L_\parallel T^{1/2})$ where the units are $n(m^{-3})$, μ(proton mass), B(T), $L_\parallel$(m) and T(eV). If we take typical values near the last closed flux surface (LCS), T = 30 eV, $L_\parallel = qR$ and $\mu = 2$, we obtain

$$n_{e0} = 1.31\times 10^{20}\,\frac{B}{qR} \tag{2}$$

This is similar to the well-known Greenwald-Hugill density limit[6,7] for the *average* density of a (here circular) plasma, where the coefficient $1.31 \rightarrow 1.6$. The correspondence requires that near the density limit the density at the LCS becomes comparable to the average density, i.e. the profile must become broad. While the T scalings are not identical, the departure in LCS temperature from 30 eV between different machines and operating conditions is small compared with the variations in B/qR.

The formal derivation is based on the vorticity and continuity equations, Ohm's and Ampere's laws and sheath boundary conditions in the SOL. These equations involve the electrostatic potential ϕ, the density n, the current $J_\parallel$ and vector potential $A_\parallel$. Next, we employ an ansatz to eliminate the dimension along the field lines

$$\phi = \phi_0 - \psi z^2 / L^2 \tag{3}$$

where z is the coordinate in the parallel direction and ϕ_0 and ψ are functions of the perpendicular coordinates x and y. Neglecting polarization drifts, the resulting equations may be written in the dimensionless form

$$n\phi - n\psi = q\frac{\partial n}{\partial y} \tag{4}$$

$$\nabla_\perp^2 \psi = -\frac{q}{4}\frac{\partial^2 n}{\partial t \partial y} \tag{5}$$

$$\frac{\partial n}{\partial t} + e_z \cdot \nabla\phi \times \nabla n = -\alpha n \tag{6}$$

where the normalizations are as follows: n to n_{e0} of Eq. (2), ϕ and ψ to e/T, space and time to ρ_s and Ω_i respectively. In Eqs. (4)-(6) and following the subscript 0 on ϕ_0 is suppressed. Here the toroidal curvature is $-\mathbf{e}_x/R$ and $q = L_\parallel/R$. Equation (4) is the vorticity equation which balances sheath currents on the left with the pressure-weighted curvature on the right. Here $p = 2nT$ with T = const. Equation (5) is Ampere's law combined with the expression for the sheath current, while Eq. (6) is the continuity equation including parallel particle loss given by $\alpha = 2\sqrt{2}\rho_s/L_\parallel$. For densities well below the density limit, $n << 1$, ψ can be neglected and Eqs. (4) and (6) reduce to the electrostatic (ES) blob model considered in Refs. 1 and 2.

Neglecting the small α term in Eq. (6) (which describes blob decay but is not important for blob convection), the *only* parameters in this model are the value of the density (normalized to the density limit) and q. Thus, any predicted "density limit" phenomena have a degree of universality built in.

For a preliminary examination of the role of EM effects, our 2D equations are reduced[8] to 1D (in the radial coordinate x) by projecting onto two Fourier modes $k_y = 0$ and k. Letting $n = \bar{n} + \tilde{n}\cos ky$, etc. and $\tilde{g} = \tilde{\psi}_y$ yields

$$\frac{\partial \bar{n}}{\partial t} + \frac{\partial}{\partial x}\left(\frac{k^2 q \tilde{n}^2}{2\bar{n}} - \frac{1}{2}\tilde{n}\tilde{g}\right) = -\alpha\bar{n} \tag{7}$$

$$\frac{\partial \tilde{n}}{\partial t} + \frac{k^2 q}{\bar{n}}\frac{\partial \bar{n}}{\partial x}\tilde{n} - \frac{\partial \bar{n}}{\partial x}\tilde{g} = -\alpha\tilde{n} \tag{8}$$

$$\nabla_\perp^2 \tilde{g} = \frac{k^2 q}{4}\frac{\partial \tilde{n}}{\partial t} \tag{9}$$

Even this simple model retains the physics of convecting blobs. In particular, considering the ES limit n, g << 1, the ansatz $\tilde{n} = 2^{1/2}\bar{n}$ solves Eqs. (7) and (8) for an arbitrary function n(x−vt), where the blob velocity $v = k^2 q$ is in agreement with the Gaussian blob solution of Ref. 2 if we identify $k = 1/r_b$ with r_b the Gaussian blob radius.

The 1D system possesses a scaling invariance which is exhibited by the transformation $t' = \alpha t$, $x' = \alpha x/(k^2 q)$, $\tilde{g}' = \tilde{g}/(k^2 q)$, $\bar{n}' = \bar{n}k^4 q^2/\alpha$, $\tilde{n}' = \tilde{n}k^4 q^2/\alpha$, and $k' = k^3 q/\alpha$. The primed variables (with primes suppressed) are employed in the results which follow.

The 1D scaled equations have an exact steady state exponential solution, $\bar{n} = \bar{n}_0 \exp(-x)$ which balances radial convection and parallel losses. This solution describes an ensemble of radially convecting blobs, each of which decays at a rate exp(–t′) in its own frame, to give rise to an overall exponentially decaying profile. The characteristic SOL scale length is k^2q/α in the original variables. Note that although the solution is a "equilibrium" solution of the 1D model, both $\tilde{n}$ and $\bar{n}$ are involved. The solution is not independent of y.

Although the exponential solution solves the system for all value of $\bar{n}_0$, a detailed analysis shows that this solution is only stable for small $\bar{n}_0$. To explore this, we have time evolved Eqs. (7) – (9) numerically until a steady state results. Figure 1 shows an example of the results for two different separatrix densities. In the low density case, the single SOL exponential solution is recovered. In the higher density case, a double-scale-length SOL solution results. In the steep inner SOL, this solution is diffusion dominated (a small diffusion term is added to the equations for numerical evolution), while in the outer broad SOL, convection dominates. At even higher densities, an MHD unstable regime is eventually encountered.

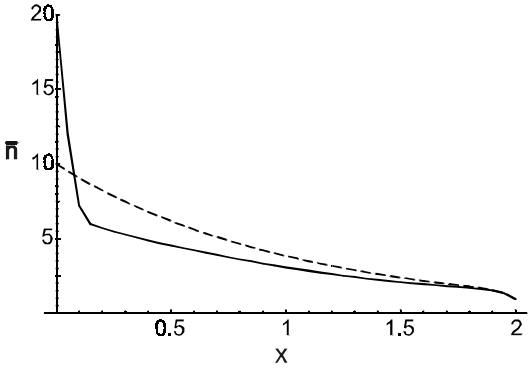

Fig. 1 Steady state solutions of the model Eqs. (7) – (9) for two values of separatrix density n_0.

We have also studied the response of the system to time-dependent forcing terms of the form $\bar{n}_0 = \bar{n}_{00}(1 + A\cos\omega t)$ applied at the separatrix boundary. When $\bar{n}_{00}$ is well below the critical density, the plasma response is rather linear looking, as seen in Fig. 2a) for the density $\bar{n}(t)$. In this figure, the time histories are shown at four fixed spatial locations (probes). The flux $\Gamma = \bar{n}v$, not shown, is similar to the density since v = 1 in this case. As $\bar{n}_{00}$ approaches a critical density, strong nonlinearities appear in the responses shown in Figs. 2b) and 2c). The flux becomes spiky, and the density shows a marked steepening of the leading edge. The first oscillation arrives nearly simultaneously (v >> 1) on all probes in Fig. 2b) while there is a measurable time delay (consistent with v = 1) in Fig. 2a). Although convection is transiently enhanced, there is no increase in the time-averaged radial fluxes because v is suppressed below 1 for part of the cycle.

Note that in the dimensionless units of this paper the MHD stability parameter is $\alpha_{mhd} = nq/L_n$ thus $\alpha_{mhd} = 1$ implies $n = 1/kq$ if $L_n \to 1/k$ gives the characteristic length scale of an isotropic blob. In the present model, we can interpret the density limit as an MHD instability limit for *blobs* or turbulent structures as opposed to the *average* SOL profiles.

Finally, it can be shown that Eq. (7) – (9) possess an analytic 1D shock solution in which $\bar{n}$ and $\tilde{n}$ jump discontinuously at the shock front while g is continuous. The shock velocity is

$$u = \frac{k^2 q}{1 - kqN/8} \tag{10}$$

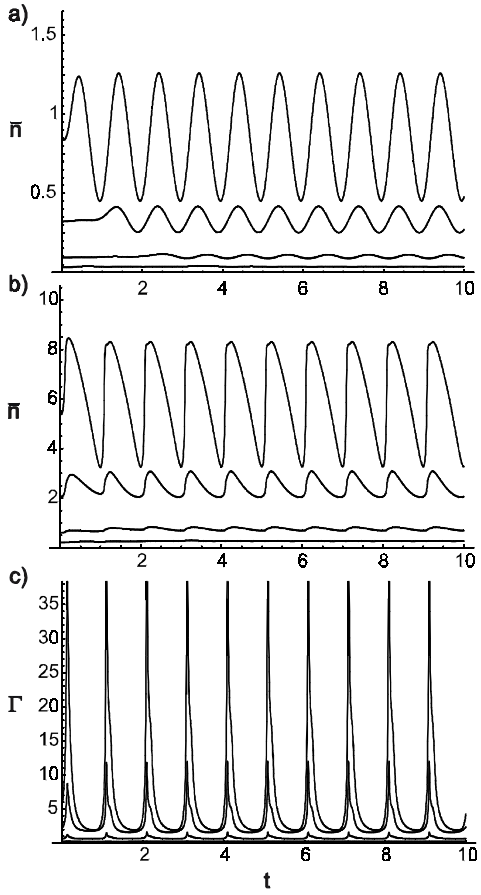

Fig. 2 Response of the plasma to a sinusoidal driving perturbation. a) $\bar{n}(t)$ for the low density case, b) $\bar{n}(t)$ for the high density case, and c) flux $\Gamma(t)$ for the high density case.

where N is the density jump. This solution shows the existence of a critical density where the convective velocity becomes large.

The singular change in character of the solutions seen in Figs. 1 and 2 near a critical density is likely associated with the absence of the polarization drift term in the corresponding 1D model equations. We are presently investigating the solutions of the full 2D equations retaining the polarization drifts. So far, we have not seen any signatures of a density limit in the 2D simulations. Work in progress is investigating the role of the polarization drift term in these findings.

It is interesting that the density limit scaling arises naturally from the model when (i) the polarization drift term is neglected, and (ii) the natural time and space scales are Ω_i and ρ_s. Is it possible to simultaneously satisfy these requirements? One hope would seem to be in nonlinear solutions which annihilate the polarization drift term. Convecting structures, such as shocks, which are steady state in a moving frame offer the possibility of cancellation of the $\partial/\partial t$ and $\mathbf{v}\cdot\nabla$ terms

In conclusion, we have investigated the role of electromagnetic effects on blob convection in the SOL and its relation to the density limit. The model produces qualitative effects which are reminiscent of the experimentally observed phenomena of increased convection, intermittency, and a double-scale-length SOL, as the density limit is approached. However, in its present form, the model exhibits interesting behaviors at critical densities which greatly exceed the density limit unless the scales sizes of the blobs are ρ_s and Ω_i. In that case the neglect of the polarization drift must be justified. Nonetheless, it is hoped that the model may contain some of the correct physical ingredients necessary for an eventual understanding of the density limit.

This work was supported by the U.S. Department of Energy (DOE) under grants DE-FG03-97ER54392 and DE-FG03-00ER54568.

1 S. I. Krasheninnikov, Phys. Lett. A. **283**, 368 (2001).
2 D. A. D'Ippolito, J. R. Myra, and S. I. Krasheninnikov, Phys. Plasmas **9**, 222 (2002).
3 B. A. Carreras, V. E. Lynch, and B. LaBombard, Phys. Plasmas **8**, 3702 (2001).
4 B. LaBombard, R. L. Boivin, M. Greenwald et al., Phys. Plasmas **8**, 2107 (2001).
5 A. V. Nedospasov, Fiz. Plazmy **15**, 1139 (1989) [Sov. J. Plasma Phys. **15**, 659 (1989)].
6 M. Greenwald, J. L. Terry, S. M. Wolfe,et al., Nucl. Fusion **28**, 2199 (1988).
7 S.J. Fielding, J. Hugill, G.M. McCracken, et al., Nucl. Fusion **17**, 1382 (1977).
8 S. Benkadda, et al., Nucl. Fusion **41**, 995 (2001).